Editors' Suggestion

Challenging Spontaneous Quantum Collapse with the XENONnT Dark Matter Detector

E. Aprile,[1] J. Aalbers,[2] K. Abe,[3] S. Ahmed Maouloud,[4] L. Althueser,[5] B. Andrieu,[4] E. Angelino,[6,7] D. Antón Martin,[8] S. R. Armbruster,[9] F. Arneodo,[10] L. Baudis,[11] M. Bazyk,[12] L. Bellagamba,[13] R. Biondi,[9,14] A. Bismark,[11,*] K. Boese,[9] A. Brown,[15] G. Bruno,[12] R. Budnik,[14] C. Cai,[16] C. Capelli,[11] J. M. R. Cardoso,[17] A. P. Cimental Chávez,[11] A. P. Colijn,[18] J. Conrad,[19] J. J. Cuenca-García,[11] V. D'Andrea,[7,†] L. C. Daniel Garcia,[4] M. P. Decowski,[18] A. Deisting,[20] C. Di Donato,[21,7] P. Di Gangi,[13] S. Diglio,[12] K. Eitel,[22] S. el Morabit,[18] A. Elykov,[22] A. D. Ferella,[21,7] C. Ferrari,[7] H. Fischer,[15] T. Flehmke,[19] M. Flierman,[18] W. Fulgione,[6,7] C. Fuselli,[18] P. Gaemers,[18] R. Gaior,[4] M. Galloway,[11] F. Gao,[16] S. Ghosh,[23] R. Giacomobono,[24] F. Girard,[4] R. Glade-Beucke,[15] L. Grandi,[8] J. Grigat,[15] H. Guan,[23] M. Guida,[9] P. Gyorgy,[20] R. Hammann,[9] A. Higuera,[25] C. Hils,[20] L. Hoetzsch,[9] N. F. Hood,[26] M. Iacovacci,[24] Y. Itow,[27] J. Jakob,[5] F. Joerg,[11] Y. Kaminaga,[3] M. Kara,[22] P. Kavrigin,[14] S. Kazama,[27] P. Kharbanda,[18] M. Kobayashi,[27] D. Koke,[5] A. Kopec,[26,‡] H. Landsman,[14] R. F. Lang,[23] L. Levinson,[14] I. Li,[25] S. Li,[28] S. Liang,[25] Z. Liang,[28] Y.-T. Lin,[9] S. Lindemann,[15] K. Liu,[16] M. Liu,[1,16] J. Loizeau,[12] F. Lombardi,[20] J. Long,[8] J. A. M. Lopes,[17,§] G. M. Lucchetti,[13] T. Luce,[15] Y. Ma,[26] C. Macolino,[21,7] J. Mahlstedt,[19] A. Mancuso,[13] L. Manenti,[10] F. Marignetti,[24] T. Marrodán Undagoitia,[9] K. Martens,[3] J. Masbou,[12] S. Mastroianni,[24] A. Melchiorre,[21,7] J. Merz,[20] M. Messina,[7] A. Michael,[5] K. Miuchi,[29] A. Molinario,[6] S. Moriyama,[3] K. Morå,[1] Y. Mosbacher,[14] M. Murra,[1] J. Müller,[15] K. Ni,[26] U. Oberlack,[20] B. Paetsch,[14] Y. Pan,[4] Q. Pellegrini,[4] R. Peres,[11] C. Peters,[25] J. Pienaar,[8,14] M. Pierre,[18] G. Plante,[1] T. R. Pollmann,[18] L. Principe,[12] J. Qi,[26] J. Qin,[25] D. Ramírez García,[11] M. Rajado,[11] A. Ravindran,[12] A. Razeto,[7] L. Redard-Jacot,[11] R. Singh,[23] L. Sanchez,[25] J. M. F. dos Santos,[17] I. Sarnoff,[10] G. Sartorelli,[13] J. Schreiner,[9] P. Schulte,[5] H. Schulze Eißing,[5] M. Schumann,[15] L. Scotto Lavina,[4] M. Selvi,[13] F. Semeria,[13] P. Shagin,[20] S. Shi,[1] J. Shi,[16] M. Silva,[17] H. Simgen,[9] A. Stevens,[15] C. Szyszka,[20] A. Takeda,[3] Y. Takeuchi,[29] P.-L. Tan,[19,1] D. Thers,[12] G. Trinchero,[6] C. D. Tunnell,[25] F. Tönnies,[15] K. Valerius,[22] S. Vecchi,[30] S. Vetter,[22] F. I. Villazon Solar,[20] G. Volta,[9] C. Weinheimer,[5] M. Weiss,[14] D. Wenz,[5] C. Wittweg,[11,‖] V. H. S. Wu,[22] Y. Xing,[12] D. Xu,[1] Z. Xu,[1] M. Yamashita,[3] L. Yang,[26] J. Ye,[31] L. Yuan,[8] G. Zavattini,[30] and M. Zhong,[26]

(XENON Collaboration)[¶]

C. Curceanu,[32,33] S. Manti,[32] and K. Piscicchia[34,32,**]

[1]*Physics Department, Columbia University, New York, New York 10027, USA*
[2]*Nikhef and the University of Groningen, Van Swinderen Institute, 9747AG Groningen, Netherlands*
[3]*Kamioka Observatory, Institute for Cosmic Ray Research, and Kavli Institute for the Physics and Mathematics of the Universe (WPI), University of Tokyo, Higashi-Mozumi, Kamioka, Hida, Gifu 506-1205, Japan*
[4]*LPNHE, Sorbonne Université, CNRS/IN2P3, 75005 Paris, France*
[5]*Institut für Kernphysik, University of Münster, 48149 Münster, Germany*
[6]*INAF-Astrophysical Observatory of Torino, Department of Physics, University of Torino and INFN-Torino, 10125 Torino, Italy*
[7]*INFN-Laboratori Nazionali del Gran Sasso and Gran Sasso Science Institute, 67100 L'Aquila, Italy*
[8]*Department of Physics, Enrico Fermi Institute and Kavli Institute for Cosmological Physics, University of Chicago, Chicago, Illinois 60637, USA*
[9]*Max-Planck-Institut für Kernphysik, 69117 Heidelberg, Germany*
[10]*New York University Abu Dhabi - Center for Astro, Particle and Planetary Physics, Abu Dhabi, United Arab Emirates*
[11]*Physik-Institut, University of Zürich, 8057 Zürich, Switzerland*
[12]*SUBATECH, IMT Atlantique, CNRS/IN2P3, Nantes Université, Nantes 44307, France*
[13]*Department of Physics and Astronomy, University of Bologna and INFN-Bologna, 40126 Bologna, Italy*
[14]*Department of Particle Physics and Astrophysics, Weizmann Institute of Science, Rehovot 7610001, Israel*
[15]*Physikalisches Institut, Universität Freiburg, 79104 Freiburg, Germany*
[16]*Department of Physics & Center for High Energy Physics, Tsinghua University, Beijing 100084, People's Republic of China*
[17]*LIBPhys, Department of Physics, University of Coimbra, 3004-516 Coimbra, Portugal*
[18]*Nikhef and the University of Amsterdam, Science Park, 1098XG Amsterdam, Netherlands*
[19]*Oskar Klein Centre, Department of Physics, Stockholm University, AlbaNova, Stockholm SE-10691, Sweden*

[20]Institut für Physik & Exzellenzcluster PRISMA+, Johannes Gutenberg-Universität Mainz, 55099 Mainz, Germany
[21]Department of Physics and Chemistry, University of L'Aquila, 67100 L'Aquila, Italy
[22]Institute for Astroparticle Physics, Karlsruhe Institute of Technology, 76021 Karlsruhe, Germany
[23]Department of Physics and Astronomy, Purdue University, West Lafayette, Indiana 47907, USA
[24]Department of Physics "Ettore Pancini," University of Napoli and INFN-Napoli, 80126 Napoli, Italy
[25]Department of Physics and Astronomy, Rice University, Houston, Texas 77005, USA
[26]Department of Physics, University of California San Diego, La Jolla, California 92093, USA
[27]Kobayashi-Maskawa Institute for the Origin of Particles and the Universe, and Institute for Space-Earth Environmental Research, Nagoya University, Furo-cho, Chikusa-ku, Nagoya, Aichi 464-8602, Japan
[28]Department of Physics, School of Science, Westlake University, Hangzhou 310030, People's Republic of China
[29]Department of Physics, Kobe University, Kobe, Hyogo 657-8501, Japan
[30]INFN-Ferrara and Dip. di Fisica e Scienze della Terra, Università di Ferrara, 44122 Ferrara, Italy
[31]School of Science and Engineering, The Chinese University of Hong Kong (Shenzhen), Shenzhen, Guangdong 518172, People's Republic China
[32]Laboratori Nazionali di Frascati, INFN, Frascati, Italy
[33]IFIN-HH, Institutul National pentru Fizica si Inginerie Nucleara Horia Hulubei, Măgurele, Romania
[34]Centro Ricerche Enrico Fermi—Museo Storico della Fisica e Centro Studi e Ricerche "Enrico Fermi," Rome, Italy

(Received 16 June 2025; accepted 22 January 2026; published 23 March 2026)

We report on the search for x-ray radiation as predicted from dynamical quantum collapse with low-energy electronic recoil data in the energy range of 1–140 keV from the first science run of the XENONnT dark matter detector. Spontaneous radiation is an unavoidable effect of dynamical collapse models, which were introduced as a possible solution to the long-standing measurement problem in quantum mechanics. The analysis utilizes a model that for the first time accounts for cancellation effects in the emitted spectrum, which arise in the x-ray range due to the opposing electron-proton charges in xenon atoms. New world-leading limits on the free parameters of the Markovian continuous spontaneous localization and Diósi-Penrose models are set, improving previous best constraints by two orders of magnitude and a factor of five, respectively. For the strength and correlation length of the continuous spontaneous localization model, values in the originally proposed parameter ranges are experimentally excluded for the first time.

DOI: 10.1103/2jm3-4976

One of the greatest mysteries of quantum mechanics is how classical behavior emerges from the quantum realm. The superposition principle has been experimentally verified at the microscopic level with extreme precision [1], but superpositions of macroscopic states are not observed. Moreover, the mechanism that triggers the quantum-to-classical transition is not encoded in quantum mechanics. This *measurement problem* has led to the development of consistent phenomenological theories that account for the progressive breakdown of quantum superpositions as the size and complexity of a system increase. Dynamical collapse models (DCMs) consist of nonlinear and stochastic modifications of the Schrödinger equation, which require the introduction of phenomenological parameters, in such a way that the collapse rate results to be extremely small for microscopic objects, but an amplification mechanism ensures localization at the macroscopic level. The modified dynamics result in a Brownian-like diffusion of quantum systems in space during which charged particles emit *spontaneous electromagnetic radiation*. DCMs have been tested using interferometry [2,3], by measuring the heating of astrophysical objects [4] and by trying to detect indirect effects of collapse dynamics using systems such as cold atoms [5], optomechanical devices [6,7], phonon excitations in crystals [8], and gravitational wave detectors [9–12]. Moreover, searches for spontaneous radiation in the form of x-rays or γ rays have been carried out with germanium detectors [13–15].

In this Letter, we report on the search for spontaneous radiation emission by xenon atoms with the XENONnT dark matter detector, as predicted by two benchmark DCM models: the continuous spontaneous localization (CSL)

*Contact author: alexander.bismark@physik.uzh.ch
†Also at INFN-Roma Tre, 00146 Roma, Italy.
‡Present address: Department of Physics and Astronomy, Bucknell University, Lewisburg, Pennsylvania, USA.
§Also at Coimbra Polytechnic—ISEC, 3030-199 Coimbra, Portugal.
‖Now at Imperial College London, Department of Physics, Blackett Laboratory, London SW7 2AZ, United Kingdom.
¶Contact author: xenon@lngs.infn.it
**Contact author: kristian.piscicchia@cref.it

[16,17] and Diósi-Penrose (DP) [18–20] models. The two models share a similar structure for the dynamical equation. In the Markovian formulation, which is investigated in this work, a white stochastic noise is assumed in time. The models are characterized by a collapse rate parameter, which sets the strength of the collapse, and a correlation length, which measures the spatial resolution of the collapse, setting the scale beyond which spatial superpositions are suppressed. The key distinction between the two models lies in their spatial correlation forms: for CSL, it is Gaussian, with an amplitude determined by the collapse strength λ and a resolution scale set by r_C. Ghirardi, Rimini, and Weber (GRW) [21] proposed values on the order of magnitude $\lambda^{\mathrm{GRW}} \simeq 10^{-16}$ s^{-1} and $r_C^{\mathrm{GRW}} \simeq 10^{-7}$ m, which ensure the effective collapse of macroscopic systems.

The collapse in the DP model is linked to gravity, and the spatial correlation is proportional to the Newtonian potential. The correlation length R_0 acts as a spatial cutoff parameter to avoid a divergence in the collapse rate for pointlike particles, while the strength is given by the gravitational constant G. Theoretical upper bounds on R_0 can be set by requiring the prevention of macroscopic quantum superpositions [22] before they can be perceived. This sets the collapse timescale governed by R_0 at $\lesssim$0.01 s, the approximate time resolution of the human eye. For the model systems investigated in [22], the limits depend strongly on their size L: $R_0 \lesssim 10^3$ Å for $L \sim 1$ μm and $R_0 \lesssim 5 \times 10^6$ Å for $L \sim 10$ μm.

Spontaneous radiation searches provide the strongest experimental bounds on the model parameters R_0 of DP, as well as on the λ and r_C of CSL over a broad range of the parameter space [13–15]. At sufficiently high energies of $\mathcal{O}$(100 keV–MeV), the spontaneous radiation wavelengths λ_γ are intermediate between the nuclear and atomic length scales. With good approximation, protons would emit radiation coherently, while electrons would emit incoherently [15], leading to

$$\left.\frac{d\Gamma}{dE}\right|_t^{\mathrm{CSL,DP}} \propto E^{-1}(N_p^2 + N_e), \tag{1}$$

for the rate of the spontaneous radiation. Here, N_p and N_e are the numbers of protons and electrons in the atom while E is the photon energy for the radiation emitted. The constant of proportionality depends on the respective model parameters. Strong constraints on collapse models in the x-ray regime (19–100 keV) were previously set in Ref. [13], where the spontaneous emission from germanium atoms of the target was modeled according to the high-energy approximation as per Eq. (1). However, the phenomenology of spontaneous radiation is more complex when x-rays are considered, with λ_γ of the order of the atomic orbit dimensions. Here, coherent emission by the electrons and cancellation effects between the oppositely charged electrons and protons must be considered. The generalization of the emission rates for energies as low as 1 keV was derived in Ref. [23]. We use these results to search for spontaneous radiation emission signals in the energy range of 1–140 keV. The implementation of the theoretical framework for this analysis is described in the Supplemental Material [24].

Due to their low background, low energy threshold of ∼1 keV [29], and target mass of several tonnes, contemporary dual-phase xenon time projection chambers (TPCs) promise high sensitivities to spontaneous radiation, by using liquid xenon (LXe) both as emitter and detection medium. In these detectors, energy deposited from interactions with the xenon target atoms gives rise to prompt scintillation light and free ionization electrons. The former is directly detected as so-called S1 signal by arrays of photomultiplier tubes (PMTs) at the top and bottom of the TPC. The liberated charge is converted into a likewise detectable secondary scintillation signal (S2). For this, an electric field between a cathode and gate electrode drifts the electrons toward the top of the TPC. There, a second, stronger electric field between the gate and an anode extracts and accelerates them into the gaseous phase, resulting in electroluminescence. Pairing both signals enables the reconstruction of the deposited energy and the interaction position. The combined energy scale E is computed from the corrected scintillation signals ($cS1$, $cS2$) as $E = W(cS1/g_1 + cS2/g_2)$, where the mean energy to produce a quantum $W = 13.7$ eV/quanta [30], and the detector-specific gain constants g_1 and g_2 are considered [31]. In general, the charge-to-light ratio is larger for particle interactions with the electrons as opposed to the nucleus of the xenon atom. This enables discrimination between electronic recoil (ER) and nuclear recoil interactions [32], with the former being expected for the x-ray signatures investigated in this Letter.

The XENONnT experiment [33] features a dual-phase TPC with a sensitive LXe mass of 5.9 t, monitored by a total of 494 Hamamatsu R11410-21 PMTs [34]. It offers an unprecedentedly low ER background of (15.8 ± 1.3) events/(t × y × keV) below recoil energies of 30 keV in its first science run [29]. To suppress cosmogenic backgrounds, this experiment is located at the INFN Laboratori Nazionali del Gran Sasso in Italy, with a rock overburden providing shielding equivalent to about 3600 meters of water. Further background reduction is achieved through active tagging using a water tank surrounding the TPC, which is instrumented as a muon veto [35] and supplemented by an inner neutron veto system [36]. Moreover, an extensive radio assay campaign for the installed detector materials was performed [37] and the xenon in the detector is continuously purified from chemical and radioactive impurities [38–40].

With a few exceptions detailed below, the search for the spontaneous radiation signatures in ER data from

XENONnT follows the analysis performed in Ref. [29]. The signal reconstruction, calibration, and event selection are further detailed in Ref. [31]. Data from the first XENONnT science run (SR0), collected from July 6, 2021, to November 10, 2021, with an exposure of $1.16\,\mathrm{t}\times\mathrm{y}$ inside the $(4.37+0.14)$ t fiducial mass, is employed.

The expected signal spectra are modeled from the theoretical shapes according to Ref. [23]. Details on the signal models can be found in the Supplemental Material [24]. The detector response is modeled by a skew-Gaussian energy resolution smearing and the application of the combined efficiency of detection and event selection [29] to the signal spectra. Compared to [29], there are two differences in the efficiency modeling: First, this work considers an acceptance loss from a data-selection against accidental pairings of isolated light and charge signals that was underestimated previously. Second, the event-building efficiency, determined analogously to Ref. [41] and projected to energy space, is considered. These efficiency adjustments influence the CSL (DP) model results in the following by ∼17% (∼6%).

A total of nine components are considered in the background model. These encompass the double-β decay of ^{136}Xe, the β decays of ^{214}Pb, ^{133}Xe, and ^{85}Kr, the double-electron capture of ^{124}Xe, and the decay of $^{83\,m}$Kr via internal conversion inside the LXe target. Other backgrounds are γ rays from detector construction materials, solar neutrinos scattering off electrons, and random pairings of uncorrelated S1 and S2s, referred to as accidental coincidences (ACs). Analogously to Ref. [42], the free electron approximation in the solar neutrino spectrum used in Ref. [29] is supplemented by a stepping approximation [43], accounting for the electron binding energies. Furthermore, the relative ^{85}Kr rate uncertainty, which was previously overestimated due to an erroneous unit in the uncertainty propagation, was reduced from ∼65% to ∼22%. The impact of the adjustments to the background model compared to Ref. [29] on the results obtained in the following is $< 1\%$ for the CSL and DP models.

The fit of the combined signal and background model (H_1) to the measured data is performed in the parameter space of reconstructed energy in the range of 1–140 keV employing an unbinned maximum likelihood analogous to Refs. [29,44]. The best-fit result for the Markovian CSL model is shown in Fig. 1. The low-energy part of the signal region contains the highest rates and distinguishing features of the spontaneous emission spectra (see Supplemental Material [24]). This allows us to place stringent limits on the respective model parameters using a log-likelihood ratio test statistic and assuming asymptoticity of the likelihood [45].

For the Markovian CSL model, λ/r_C^2 does not change the spectral shape, so it can be deduced directly from the obtained fit rate multiplier when assuming a fixed initial value for λ/r_C^2. The CSL best-fit result is shown in Fig. 1, with a signal rate of 50^{+200}_{-50} events/$(\mathrm{t}\times\mathrm{y})$ and a p-value of ∼0.3. As a local discovery significance of $0.3\,\sigma$ is obtained, no significant excess is found and an upper limit of $\lambda/r_C^2 < 3.0\times10^{-3}\ \mathrm{s^{-1}\,m^{-2}}$ $(3.7\times10^{-3}\ \mathrm{s^{-1}\,m^{-2}})$ at 90% confidence level (CL) (95% CL) is derived. This constitutes an improvement over the previous best limit from the MAJORANA DEMONSTRATOR [13] by a factor of ∼135 and sets the new most stringent experimental constraint for $r_C \lesssim 10^{-5}$ m. A comparison of these limits with constraints from other experiments and theoretical considerations is given in Fig. 2. According to the log-likelihood ratio test statistic, the parameter set $(r_C^{\mathrm{GRW}} = 1\times10^{-7}\ \mathrm{m}, \lambda^{\mathrm{GRW}} = 1\times10^{-16}\ \mathrm{s^{-1}})$ deviates from the best-fit result by $9.1\,\sigma$. For the first time, this allows to experimentally exclude CSL model parameter values in the range originally proposed by GRW.

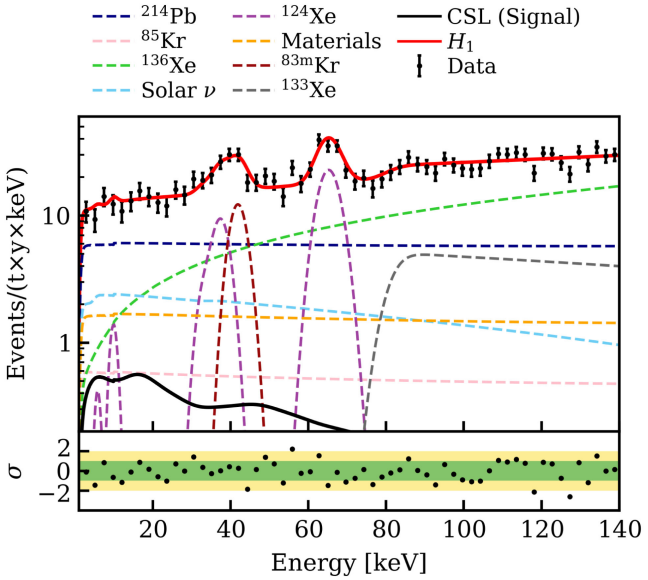

FIG. 1. Best-fit spectrum for the combined CSL signal and background model (H_1) to the XENONnT SR0 low-energy electronic recoil data. The individual background components are indicated by dashed lines, except for the subdominant AC background spectrum, which is out of range and, therefore, not shown. The best-fit result for the DP model is practically identical (see also Fig. S-1). The model discontinuity around 10 keV is due to the blinding of the dark matter search region for [46] which marginally reduces the ER rate in the data from [29] at the lowest energies.

Because of the more complex rate dependencies on the free parameter R_0 in the DP model, which can result in changes of the spectral shape beyond a global scaling, the fitting method employing a single linear rate multiplier requires an iterative approach for the DP model: A fixed starting value for R_0 and, thus, a static spectral shape are assumed. The values assumed in the next iterations are then obtained from the best-fit rate multiplier of the previous iteration by considering only a scaling by the leading term

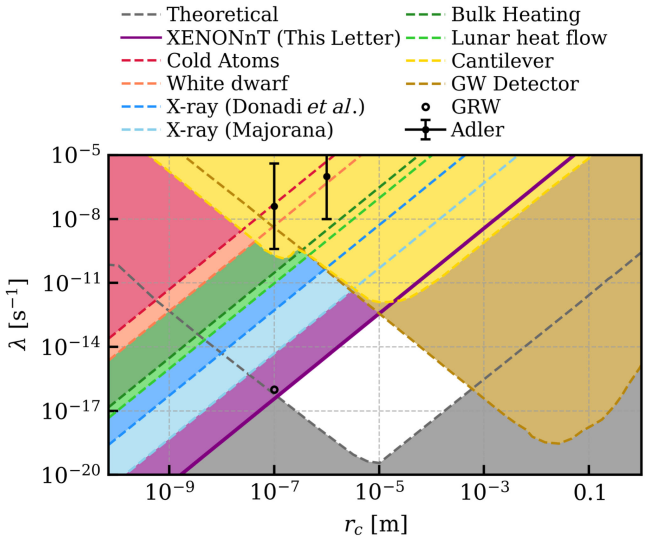

FIG. 2. XENONnT 95% CL upper bound on the CSL model parameters, compared to exclusion limits from other non-interferometric experiments and theoretical propositions, with the shaded areas marking the excluded regions of the parameter space. Results from the LISA PATHFINDER gravitational wave detector [11,12], microcantilever measurements [6], cold atoms experiments [5], and estimates from the bulk heating rate in the CUORE experiment [47] are given. The two previous best limits from x-ray emission searches by Donadi *et al.* [15] and the MAJORANA DEMONSTRATOR [13] are shown as well. Moreover, astrophysical bounds from lunar thermal emission as well as from the cooling of white dwarf J1251 + 4403 are indicated [4]. A commonly adopted lower theoretical bound can be introduced by requiring a maximum collapse time of ∼10 ms, i.e., the perception time of the human eye, for a superposition of a single-layered graphene disk of a barely visible radius of ∼10 μm [48]. The black markers indicate theoretical suggestions by Adler [49] and Ghirardi, Rimini, and Weber [50].

proportional to R_0^{-3} (see Ref. [23]). Any starting values that are not excluded by former experiments lead to the convergence to a best-fit value of $R_0 \approx 9.1 \times 10^{-10}$ m. Around this value, the spectral shape of the signal does not change significantly (see Fig. S-1 in Supplemental Material [24]), such that best-fit values, significances, and limits are in good approximation independent of the assumed R_0. With a local DP discovery significance of $0.2\,\sigma$, a lower limit of $R_0 > 4.9 \times 10^{-10}$ m (4.5×10^{-10} m) at 90% CL (95% CL) is set. This constitutes an improvement by approximately a factor of five compared to the previous world-leading limit by the MAJORANA DEMONSTRATOR [13].

In summary, new best constraints on the CSL and DP models, respectively, of $\lambda/r_C^2 < 3.0 \times 10^{-3}$ s^{-1} m^{-2} (3.7×10^{-3} s^{-1} m^{-2}) and $R_0 > 4.9 \times 10^{-10}$ m (4.5×10^{-10} m) at 90% CL (95% CL) are set. The former allows for the first-time exclusion of the commonly assumed values $(r_C^{\mathrm{GRW}}, \lambda^{\mathrm{GRW}})$ for a white noise field. The limit enhancements demonstrate the broad physics reach of the XENONnT experiment and dual-phase xenon TPCs in general. They further drive the ongoing exploration of the still feasible parameter space for the most well-studied dynamical collapse models. A wider parameter range remains to be probed for colored or dissipative model extensions [48,51]. With more XENONnT data already available, further sensitivity enhancements are expected.

We gratefully acknowledge support from the National Science Foundation, Swiss National Science Foundation, German Ministry for Education and Research, Max Planck Gesellschaft, Deutsche Forschungsgemeinschaft, Helmholtz Association, Dutch Research Council (NWO), Fundacao para a Ciencia e Tecnologia, Weizmann Institute of Science, Binational Science Foundation, Région des Pays de la Loire, Knut and Alice Wallenberg Foundation, Kavli Foundation, JSPS Kakenhi, JST FOREST Program, and ERAN in Japan, Tsinghua University Initiative Scientific Research Program, UZH Postdoc Grant (Grant No. FK-24-101), DIM-ACAV+ Région Ile-de-France, and Istituto Nazionale di Fisica Nucleare. This project has received funding/support from the European Union's Horizon 2020 research and innovation program under the Marie Skłodowska-Curie Grant Agreement No. 860881-HIDDeN. C. C., K. P. and S. M. acknowledge of the John Templeton Foundation, Grant 62099. The opinions expressed in this publication are those of the authors and do not necessarily reflect the views of the John Templeton Foundation. C. C. acknowledge support from the Foundational Questions Institute and Fetzer Franklin Fund, a donor advised fund of Silicon Valley Community Foundation (Grants No. FQXi-RFP-CPW-2008 and No. FQXi-MGB-2011), and from the INFN (VIP). C. C. benefited from the EU COST Actions CA23115 and CA23130. K. P. acknowledges support from the Centro Ricerche Enrico Fermi—Museo Storico della Fisica e Centro Studi e Ricerche "Enrico Fermi" (Open Problems in Quantum Mechanics project). We gratefully acknowledge support for provision of computing and data-processing resources of the Open Science Pool and the European Grid Initiative, at the following computing centers: the CNRS/IN2P3 (Lyon—France), the Dutch national e-infrastructure with the support of SURF Cooperative, the Nikhef Data-Processing Facility (Amsterdam—Netherlands), tfhe INFN-CNAF (Bologna—Italy), the San Diego Supercomputer Center (San Diego—USA) and the Enrico Fermi Institute (Chicago—USA). We acknowledge the support of the Research Computing Center (RCC) at The University of Chicago for providing computing resources for data analysis. We thank the INFN Laboratori Nazionali del Gran Sasso for hosting and supporting the XENON project.

Data availability—The data that support the findings of this article are not publicly available. The data are available from the authors upon reasonable request.

[1] Y. Y. Fein, P. Geyer, P. Zwick, F. Kiałka, S. Pedalino, M. Mayor, S. Gerlich, and M. Arndt, Quantum superposition of molecules beyond 25 kDa, Nat. Phys. **15**, 1242 (2019).

[2] A. Bassi, K. Lochan, S. Satin, T. P. Singh, and H. Ulbricht, Models of wave-function collapse, underlying theories, and experimental tests, Rev. Mod. Phys. **85**, 471 (2013).

[3] M. Carlesso, S. Donadi, L. Ferialdi, M. Paternostro, H. Ulbricht, and A. Bassi, Present status and future challenges of non-interferometric tests of collapse models, Nat. Phys. **18**, 243 (2022).

[4] M. M. Ocampo, M. M. Miller Bertolami, and G. León, Revisiting astrophysical bounds on continuous spontaneous localization models, J. Cosmol. Astropart. Phys. 10 (2024) 018.

[5] M. Bilardello, S. Donadi, A. Vinante, and A. Bassi, Bounds on collapse models from cold-atom experiments, Physica (Amsterdam) **462A**, 764 (2016).

[6] A. Vinante, M. Carlesso, A. Bassi, A. Chiasera, S. Varas, P. Falferi, B. Margesin, R. Mezzena, and H. Ulbricht, Narrowing the parameter space of collapse models with ultracold layered force sensors, Phys. Rev. Lett. **125**, 100404 (2020).

[7] A. Pontin, N. P. Bullier, M. Toroš, and P. F. Barker, Ultranarrow-linewidth levitated nano-oscillator for testing dissipative wave-function collapse, Phys. Rev. Res. **2**, 023349 (2020).

[8] S. L. Adler and A. Vinante, Bulk heating effects as tests for collapse models, Phys. Rev. A **97**, 052119 (2018).

[9] M. Carlesso, A. Bassi, P. Falferi, and A. Vinante, Experimental bounds on collapse models from gravitational wave detectors, Phys. Rev. D **94**, 124036 (2016).

[10] B. Helou, B. Slagmolen, D. E. McClelland, and Y. Chen, LISA Pathfinder appreciably constrains collapse models, Phys. Rev. D **95**, 084054 (2017).

[11] M. Carlesso, M. Paternostro, H. Ulbricht, A. Vinante, and A. Bassi, Non-interferometric test of the continuous spontaneous localization model based on rotational optomechanics, New J. Phys. **20**, 083022 (2018).

[12] M. Armano *et al.*, Beyond the required LISA free-fall performance: New LISA Pathfinder results down to 20 μHz, Phys. Rev. Lett. **120**, 061101 (2018).

[13] I. J. Arnquist *et al.* (MAJORANA Collaboration), Search for spontaneous radiation from wave function collapse in the MAJORANA DEMONSTRATOR, Phys. Rev. Lett. **129**, 080401 (2022); **130**, 239902(E) (2023).

[14] S. Donadi, K. Piscicchia, C. Curceanu, L. Diósi, M. Laubenstein, and A. Bassi, Underground test of gravity-related wave function collapse, Nat. Phys. **17**, 74 (2021).

[15] S. Donadi, K. Piscicchia, R. Del Grande, C. Curceanu, M. Laubenstein, and A. Bassi, Novel CSL bounds from the noise-induced radiation emission from atoms, Eur. Phys. J. C **81**, 773 (2021).

[16] P. M. Pearle, Combining stochastic dynamical state vector reduction with spontaneous localization, Phys. Rev. A **39**, 2277 (1989).

[17] G. C. Ghirardi, P. M. Pearle, and A. Rimini, Markov processes in Hilbert space and continuous spontaneous localization of systems of identical particles, Phys. Rev. A **42**, 78 (1990).

[18] L. Diosi, A universal master equation for the gravitational violation of quantum mechanics, Phys. Lett. A **120**, 377 (1987).

[19] L. Diósi, Models for universal reduction of macroscopic quantum fluctuations, Phys. Rev. A **40**, 1165 (1989).

[20] R. Penrose, On gravity's role in quantum state reduction, Gen. Relativ. Gravit. **28**, 581 (1996).

[21] G. C. Ghirardi, A. Rimini, and T. Weber, A unified dynamics for micro and MACRO systems, Phys. Rev. D **34**, 470 (1986).

[22] L. Figurato, M. Dirindin, J. L. Gaona-Reyes, M. Carlesso, A. Bassi, and S. Donadi, On the effectiveness of the collapse in the Diósi–Penrose model, New J. Phys. **26**, 113004 (2024).

[23] K. Piscicchia, S. Donadi, S. Manti, A. Bassi, M. Derakhshani, L. Diósi, and C. Curceanu, X-ray emission from atomic systems can distinguish between prevailing dynamical wave-function collapse models, Phys. Rev. Lett. **132**, 250203 (2024).

[24] See Supplemental Material at http://link.aps.org/supplemental/10.1103/2jm3-4976 for a detailed description of the signal models, which includes Refs. [25–28].

[25] C. Coulson and A. Neilson, Electron correlation in the ground state of helium, Proc. Phys. Soc. (1958–1967) **78**, 831 (1961).

[26] P. M. Gill, D. P. O'Neill, and N. A. Besley, Two-electron distribution functions and intracules, Theor. Chem. Accounts **109**, 241 (2003).

[27] W. Kohn and L. J. Sham, Self-consistent equations including exchange and correlation effects, Phys. Rev. **140**, A1133 (1965).

[28] J. J. Mortensen *et al.*, GPAW: An open Python package for electronic structure calculations, J. Chem. Phys. **160**, 092503 (2024).

[29] E. Aprile *et al.* (XENON Collaboration), Search for new physics in electronic recoil data from XENONnT, Phys. Rev. Lett. **129**, 161805 (2022).

[30] C. E. Dahl, The physics of background discrimination in liquid xenon, and first results from XENON10 in the hunt for WIMP dark matter, Ph.D. thesis, Princeton University, 2009.

[31] E. Aprile *et al.* (XENON Collaboration), XENONnT analysis: Signal reconstruction, calibration, and event selection, Phys. Rev. D **111**, 062006 (2025).

[32] E. Aprile, C. E. Dahl, L. DeViveiros, R. Gaitskell, K. L. Giboni, J. Kwong, P. Majewski, K. Ni, T. Shutt, and M. Yamashita, Simultaneous measurement of ionization and scintillation from nuclear recoils in liquid xenon as target for a dark matter experiment, Phys. Rev. Lett. **97**, 081302 (2006).

[33] E. Aprile *et al.* (XENON Collaboration), The XENONnT dark matter experiment, Eur. Phys. J. C **84**, 784 (2024).

[34] V. C. Antochi *et al.*, Improved quality tests of R11410-21 photomultiplier tubes for the XENONnT experiment, J. Instrum. **16**, P08033 (2021).

[35] E. Aprile *et al.* (XENON Collaboration), Conceptual design and simulation of a water Cherenkov muon veto for the XENON1T experiment, J. Instrum. **9**, P11006 (2014).

[36] E. Aprile *et al.* (XENON Collaboration), The neutron veto of the XENONnT experiment: Results with demineralized water, Eur. Phys. J. C **85**, 695 (2025).
[37] E. Aprile *et al.* (XENON Collaboration), Material radiopurity control in the XENONnT experiment, Eur. Phys. J. C **82**, 599 (2022).
[38] G. Plante, E. Aprile, J. Howlett, and Y. Zhang, Liquid-phase purification for multi-tonne xenon detectors, Eur. Phys. J. C **82**, 860 (2022).
[39] E. Aprile *et al.* (XENON Collaboration), Removing krypton from xenon by cryogenic distillation to the PPQ level, Eur. Phys. J. C **77**, 275 (2017).
[40] M. Murra, D. Schulte, C. Huhmann, and C. Weinheimer, Design construction and commissioning of a high-flow radon removal system for XENONnT, Eur. Phys. J. C **82**, 1104 (2022).
[41] E. Aprile *et al.* (XENON Collaboration), WIMP dark matter search using a 3.1 tonne × year exposure of the XENONnT experiment, Phys. Rev. Lett. **135**, 221003 (2025).
[42] E. Aprile *et al.* (XENON Collaboration), Detector signal characterization with a Bayesian network in XENONnT, Phys. Rev. D **108**, 012016 (2023).
[43] J.-W. Chen, H.-C. Chi, C. P. Liu, and C.-P. Wu, Low-energy electronic recoil in xenon detectors by solar neutrinos, Phys. Lett. B **774**, 656 (2017).
[44] E. Aprile *et al.* (XENON Collaboration), Excess electronic recoil events in XENON1T, Phys. Rev. D **102**, 072004 (2020).
[45] S. Baker and R. D. Cousins, Clarification of the use of chi square and likelihood functions in fits to histograms, Nucl. Instrum. Methods **221**, 437 (1984).
[46] E. Aprile *et al.* (XENON Collaboration), First dark matter search with nuclear recoils from the XENONnT experiment, Phys. Rev. Lett. **131**, 041003 (2023).
[47] C. Alduino *et al.* (CUORE Collaboration), The projected background for the CUORE experiment, Eur. Phys. J. C **77**, 543 (2017).
[48] M. Toroš, G. Gasbarri, and A. Bassi, Colored and dissipative continuous spontaneous localization model and bounds from matter-wave interferometry, Phys. Lett. A **381**, 3921 (2017).
[49] S. L. Adler, Lower and upper bounds on CSL parameters from latent image formation and IGM heating, J. Phys. A **40**, 2935 (2007); **40**, 13501(E) (2007).
[50] G. C. Ghirardi, A. Rimini, and T. Weber, Unified dynamics for microscopic and macroscopic systems, Phys. Rev. D **34**, 470 (1986).
[51] S. L. Adler and A. Bassi, Collapse models with non-white noises, J. Phys. A **40**, 15083 (2007).